^{83}Kr and ^{131}Xe nuclear quadrupole coupling and quadrupolar shielding in KrHCl and XeDCl

E. J. Campbell, L. W. Buxton, M. R. Keenan, and W. H. Flygare
Noyes Chemical Laboratory, University of Illinois, Urbana, Illinois 61801
(Received 9 March 1981)

Rotational spectra have been assigned for ^{83}KrH^{35}Cl, ^{83}KrD^{35}Cl, ^{131}XeD^{35}Cl, and ^{132}XeD^{35}Cl. Additional assignments are reported for ^{131}XeH^{35}Cl. The measured rare-gas nuclear quadrupole coupling constants χ^R are (in MHz): ^{83}KrH^{35}Cl, 5.20(10); ^{83}KrD^{35}Cl, 7.19(10); ^{131}XeH^{35}Cl, $-4.64(5)$; and ^{131}XeD^{35}Cl, $-5.89(20)$. We find that the electric field gradient along the a inertial axis at the rare-gas nuclear site in ^{83}KrH(D)F, ^{83}KrH(D)^{35}Cl, and ^{83}KrHC^{14}N, and in ^{131}XeH(D)^{35}Cl is directly proportional to the electric field gradient at that site calculated from the electric multipole moments of the partner hydrogen halide. The proportionality constants are, for ^{83}Kr, 78.5 and, for ^{131}Xe, 154, using values of 0.27×10^{-24} cm^2 and -0.12×10^{-24} cm^2 for the nuclear quadrupole moments of ^{83}Kr and ^{131}Xe, respectively. This direct proportionality is attributed to Sternheimer-type quadrupolar shielding of the rare-gas nucleus by the electrons in the rare-gas atom. Within the limits of uncertainty of this experiment of $\lesssim 0.003$ electron we find no evidence for charge transfer from the Kr atom. Although less complete, the ^{131}Xe data are also consistent with this result.

INTRODUCTION

We report the measurement and analysis of the ^{83}Kr and ^{131}Xe nuclear quadrupole coupling constants in ^{83}KrH^{35}Cl, ^{83}KrD^{35}Cl, and ^{131}XeD^{35}Cl. The rare-gas nuclear quadrupole coupling is observed through the coupling of the nuclear angular momentum to the rotational angular momentum of the molecule as measured in the vibrational ground state, pure rotational transitions of KrH(D)Cl and XeDCl. The rotational spectrum is observed by using the newly developed experimental method of pulsed Fourier-transform microwave spectroscopy in a Fabry-Perot cavity with a pulsed supersonic gas expansion.[1-4] Because the nuclear quadrupole coupling constant of the closed-shell free rare-gas atom is identically zero, the effect measured here arises from a distortion of the spherical symmetry of the atom upon complexation. We thus have a sensitive probe for studying small changes in the electronic environment of the rare-gas nucleus that occur when the rare-gas atom binds to the hydrogen halide molecule. Since our report[5] of the first measurement of a rare-gas nuclear quadrupole coupling constant in the ^{83}KrHF van der Waals molecule, we have reported similar measurements in ^{131}XeH^{35}Cl (Ref. 6) and ^{83}KrDF (Ref. 7). These studies have established, based on calculated values of the Sternheimer quadrupole shielding constants[8-10] for Kr and Xe, that most of the magnitude of the rare-gas quadrupole coupling constant in each of these molecules can be attributed to quadrupole shielding effects occurring in the rare-gas atom in the presence of the electron field gradient of the partner hydrogen halide molecule. By combining our experimental results for ^{83}Kr(D)F with the ^{83}KrH(D)^{35}Cl measurements reported here, we establish this result empirically for Kr, thereby obtaining an experimental estimate for the Sternheimer parameter for this atom. We also report an improved measurement of the Xe nuclear quadrupole coupling constant in ^{131}XeH^{35}Cl and show that our results for ^{131}XeH(D)^{35}Cl are consistent with the interpretation used for the Kr containing species.

EXPERIMENTAL

The experimental technique used here is the method of pulsed Fourier-transform microwave spectroscopy carried out in a Fabry-Perot cavity with a pulsed supersonic nozzle gas expansion.[1-4] The source gas for the nozzle consisted of mixtures of 0.3 to 1.1 mol% HCl or DCl with 70 to 80 at.% He and 20 to 30 at.% Xe or Kr at pressures ranging from 0.17 to 2.5 atm. A pulsed solenoid valve with a 0.040-inch-diameter orifice plate was used to pulse the gas into the cavity at repetition rates of about 1 Hz. Careful optimization of the gas mixture and source conditions was crucial for obtaining an adequate signal-to-noise ratio. When the expanding gas, which is now at temperatures of 1–10 K and contains large numbers of weakly bound molecular complexes, passes between the Fabry-Perot mirrors a $\pi/2$ microwave pulse is used to polarize all rotational transitions within the bandwidth of the cavity. After the polarizing radiation dies away these polarized rotational transitions emit coherently at their resonance frequencies. This coherence decays because of Doppler effects, molecular collisions, and the molecular transit out of the

cavity. The decaying molecular emission is coupled out of the cavity and detected in a superheterodyne receiver by mixing with a local oscillator. The signal is digitized and stored to be averaged with the signals from repreating gas pulses. After an adequate signal-to-noise ratio is obtained, the time domain signal is Fourier transformed into the frequency domain. In the case of a single resonance frequency, the gas flow from the nozzle and the resultant Doppler effect gives rise to a symmetric doublet in the frequency domain. The gas dynamics of the pulsed nozzle, the molecular polarization and subsequent emission processes, and the characteristic Doppler-doubling phenomenon have been described in more detail elsewhere.[11,12]

Most of the data presented here for molecules containing two interacting nuclear quadrupole moments were taken at frequencies below 8 GHz.[13] Because the Doppler splitting in the frequency domain is proportional to the resonance frequency, at these lower frequencies the two Doppler peaks become merged. This simplifies the spectrometer signals and doubles the signal-to-noise ratio. Furthermore, the quadrupole splitting patterns are simplified and better resolved at lower values of the angular-momentum quantum number J. The deuterium nuclear quadrupole splittings remained unresolved, causing the resonance lines to broaden. In Fig. 1 we show a power spectrum containing the $J=1\rightarrow 2$, $F_1=\frac{5}{2}$, $F_2=7$, $F=8\rightarrow F_1'=\frac{7}{2}$, $F_2'=8$, $F'=9$ and $F_1=\frac{5}{2}$, $F_2=6$, $F=5\rightarrow F_1'=\frac{7}{2}$, $F_2'=7$, $F'=8$ lines of ^{83}KrD^{35}Cl. The spectrum was obtained by averaging 30 emission signals, weighting the resultant time domain record with a digital exponential filter, and taking the power spectrum. In Fig. 2 we show a portion of the calculated pattern in the frequency domain of the ^{83}KrD^{35}Cl $J=1\rightarrow 2$ transition. The envelope was generated from the measured values of the ^{83}Kr and ^{35}Cl nuclear quadrupole coupling constants, and the calculated projection of the deuterium quadrupole coupling constant in free D^{35}Cl. The nine resonance lines reported here are represented as vertical bars. The assignments are identified in Table II.

ROTATIONAL SPECTRA AND SPECTROSCOPIC CONSTANTS

The rotational energy levels for ^{83}KrH(D)^{35}Cl and ^{131}XeH(D)^{35}Cl are determined by the $K=0$ symmetric-top Hamiltonian[14]

$$\frac{1}{h}H(\vec{J},\vec{I}_{Cl},\vec{I}_R,\vec{I}_D,\vec{F}_1,\vec{F}_2,\vec{F})=\bar{B}_0\vec{J}^2-D_J\vec{J}^4-\sum_i\frac{\chi_i[3(\vec{I}_i\cdot\vec{J})^2+\frac{3}{2}(\vec{I}_i\cdot\vec{J})-\vec{I}_i^2\vec{J}^2]}{2I_i(2I_i-1)(2J-1)(2J+3)}, \tag{1}$$

where $\bar{B}_0=\frac{1}{2}(B_0+C_0)$ is the rotational constant, D_J is the centrifugal distortion constant, and χ_i and I_i, $i=1,2,3$, are the chlorine, rare-gas, and deuterium nuclear quadrupole coupling constants and nuclear spins, as necessary. Matrix elements of this Hamiltonian were calculated to first order in the basis

$$\begin{aligned}&\vec{J}+\vec{I}_{Cl}=\vec{F}_1,\\&\vec{F}_1+\vec{I}_R=\vec{F}_2,\\&\vec{F}_2+\vec{I}_D=\vec{F},\end{aligned} \tag{2}$$

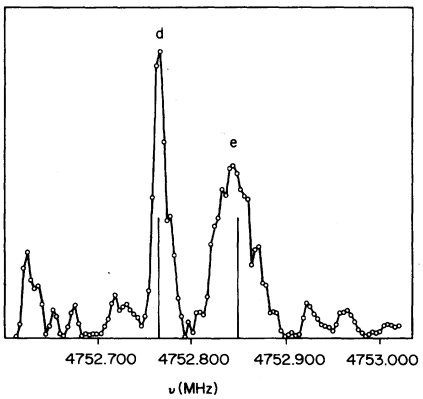

FIG. 1. Power spectrum showing the $J=1\rightarrow 2$, $F_1=\frac{5}{2}$, $F_2=7$, $F=8\rightarrow F_1'=\frac{7}{2}$, $F_2'=8$, $F'=9$, and $F_1=\frac{5}{2}$, $F_2=6$, $F=5\rightarrow F_1'=\frac{7}{2}$, $F_2'=7$, $F'=8$ lines of ^{83}KrD^{35}Cl at 4.7 GHz. Both the deuterium nuclear quadrupole splittings and the Doppler splittings are unresolved. This spectrum was taken in approximately one minute.

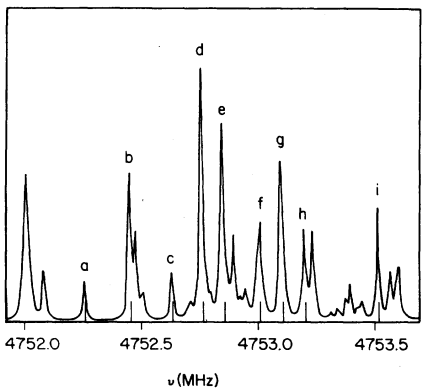

FIG. 2. Calculated envelope and the measured transitions for the ^{83}KrD^{35}Cl $J=1\rightarrow 2$ multiplet. The assignments are identified in Table II.

TABLE I. Observed and calculated frequencies for $^{83}KrH^{35}Cl$.

$J \rightarrow J'$	$2F_1$	$2F$	$2F_1'$	$2F'$	Observed (MHz)	Calculated (MHz)	Difference (kHz)
1 2	1	10	1	10	4819.3741	4819.3689	5.2
	1	10	1	8			
	1	8	1	10			
	1	8	1	8			
	3	12	5	14	4819.6873	4819.6885	−1.2
	5	14	7	16	4819.9086	4819.9061	2.5
	5	12	7	14	4819.9687	4819.9719	−3.2
	5	10	7	12	4820.1545	4820.1524	2.1
	5	8	7	10	4820.2222	4820.2217	0.5
	3	8	5	8	4820.2581	4820.2459	12.2
	5	6	7	8			
	3	12	3	10	4825.0474	4825.0454	2.0
	3	12	3	12	4825.0872	4825.0878	−0.6
	3	8	3	10	4825.4199	4825.4184	1.5
	3	8	3	6	4825.4681	4825.4714	−3.3
	3	10	3	10	4825.5646	4725.5705	−5.9
	3	10	3	8	4825.5912	4825.5857	5.5

where the subscript R indicates either Kr or Xe. The $^{131}XeH^{35}Cl$ data were fit with energy levels calculated from Eq. (1) only to first order. Small second-order chlorine nuclear quadrupole effects in the $^{83}KrH(D)^{35}Cl$, $^{131}XeD^{35}Cl$, and $^{132}XeD^{35}Cl$ spectra were taken into account by adjusting the appropriate energy levels obtained from the first-order evaluation of Eq. (1) by amounts corresponding to the second-order corrections obtained by direct diagonalization of the single chlorine quadrupole Hamiltonian. Except in the case of the $F_1 = \frac{3}{2} \rightarrow F_1' = \frac{3}{2}$ series of transitions in $^{83}KrH^{35}Cl$, where a second-order shift of 9 kHz did affect the fit to χ^{Cl}, and in $^{132}XeD^{35}Cl$, second-order shifts were 4 kHz or less. Calculated line positions for all deuterium-containing molecules were obtained as weighted averages of all unresolved components estimated to contribute to the corresponding measured frequencies. Since some of these lines consisted of up to ten unresolved hyperfine lines, the assignments are in certain cases identified only by the first, last, and largest contributing components. The observed spectra, their assignments, calculated frequencies, and frequency differences, are listed in Tables I–V. The spectroscopic constants used to fit the data are shown in Tables VI and VII. The spectroscopic constants of $^{83}KrHC^{14}N$, taken from a report on the microwave spectrum and structure of this molecule,[15] are listed in Table VIII. The structural parameters, R_0, the distance between the rare-gas nucleus and the center of mass of the hydrogen halide, and θ, the angle formed by the rare gas, the center mass of the hydrogen

TABLE II. Observed and calculated frequencies for $^{83}KrD^{35}Cl$.

$J \rightarrow J'$		$2F_1$	$2F_2$	$2F$	$2F_1'$	$2F_2'$	$2F$	Observed (MHz)	Calculated (MHz)	Difference (kHz)
1 2	a	3	6	4	5	6	4	4752.2616	4752.2591	2.5
	b	3	12	14	5	14	16	4752.4514	4752.4565	−5.1
	c	5	4	6	7	2	4	4752.6426	4752.6366	6.0
	d	5	14	16	7	16	18	4752.7641	4752.7656	−1.5
	e	5	12	10	7	14	12	4752.8492	4752.8545	−5.3
		5	12	14	7	14	16			
		5	10	10	7	14	12			
	f	3	8	8	5	6	6	4753.0063	4753.0087	−2.4
		5	10	8	7	10	8			
		5	12	12	7	10	12			
	g	5	10	12	7	12	14	4753.1106	4753.1061	4.5
		5	10	8	7	12	10			
		5	10	10	7	12	12			
	h	5	8	10	7	10	12	4753.1979	4753.2012	−3.3
	i	3	10	12	5	12	14	4753.5214	4753.5171	4.3

TABLE III. Observed and calculated frequencies for ^{132}XeD^{35}Cl.

$J \rightarrow J'$	$2F_1$	$2F$	$2F_1'$	$2F'$	Observed (MHz)	Calculated (MHz)	Difference (kHz)
2 3	3	3	5	3	5844.4185	5844.4193	−0.8
	1	3	3	5			
	3	3	5	5			
	5	3	7	5	5847.2103	5847.2113	−1.0
	7	9	9	11			
	5	5	7	7			
4 5	5,7		7,9		9742.8321	9742.8317	0.4
	9,11		11,13		9743.6026	9743.6019	0.7
6 7	9,11		11,13		13638.1782	13638.1785	−0.3
	13,15		15,17		13638.5446	13638.5462	−1.6
7 8	11,13		13,15		15584.9467	15584.9441	2.6
	15,17		17,19		15585.2218	15585.2212	0.6
8 9	13,15		15,17		17531.0287	17531.0308	−2.1
	17,19		19,21		17531.2472	17531.2473	−0.1

halide, and the hydrogen (deuterium), are listed for KrHCl and XeDCl in Table IX. These structural parameters are shown in Fig. 3. The angle formed by γ between the a inertial axis and the hydrogen halide bond is obtained in the usual way[2] by assuming that the measured value of χ^{Cl} is given by the projection of the chlorine nuclear quadrupole coupling constant χ_0^{Cl} of free $H^{35}Cl$ onto the a inertial axis according to

$$\chi^{Cl} = \chi_0^{Cl} \left\langle \frac{3\cos^2\gamma - 1}{2} \right\rangle , \tag{3}$$

where the brackets indicate averaging over the ground vibrational state of the complex. If the hydrogen halide bond length r remains unchanged upon complexation, then R_0 and θ may be obtained from γ and the rotational constant $\overline{B}_0$. The assumption here regarding r, and the assumption that the change in χ^{Cl} from χ_0^{Cl} is purely a geometrical effect and does not involve any changes in the electronic environment of the chlorine nucleus can be tested experimentally,[16,17] and are found to be correct for the rare-gas hydrogen halides within experimental error. The structural analysis for KrHCN is similar, using the projection of the ^{14}N nuclear quadrupole coupling constant. The structural parameters for this molecule are shown in Fig. 4.

ANALYSIS

The rare-gas nuclear quadrupole coupling constant χ is determined by the product of the quadrupole moment Q of the rare-gas nucleus and the electric field gradient q at the nuclear site along the molecular a inertial axis due to all charges outside the nucleus. χ is given by

$$\chi = -\frac{eqQ}{h} , \tag{4}$$

where e is the proton charge and h is Planck's constant. Since the quadrupole moments of the ^{83}Kr and ^{131}Xe nuclei have been determined to approximately 15% accuracy by atomic hyperfine structure measurements, the problem of evaluating χ reduces to determining q. Direct calcula-

TABLE IV. Observed and calculated frequencies for ^{131}XeH^{35}Cl.

$J \rightarrow J'$	$2F_1$	$2F$	$2F_1'$	$2F'$	Observed (MHz)	Calculated (MHz)	Difference (kHz)
1 2	5	6	7	8	3963.9586	3963.9587	−0.1
	5	4	7	6	3964.0333	3964.0335	−0.2
	5	8	7	10	3964.1764	3964.1749	1.5
	3	6	5	8	3964.3899	3964.3911	−1.2
2 3	5	6	7	8	5944.9615	5944.9625	−1.0
	7	6	9	8	5945.0682	5945.0703	−2.1
	5	4	7	6			
	7	8	9	10	5945.1475	5945.1482	−0.7
	7	4	9	6			
	7	10	9	12	5945.2383	5945.2373	1.0
	5	8	7	10	5945.3294	5945.3297	−0.3

TABLE V. Observed and calculated frequencies for $^{131}XeD^{35}Cl$.

$J \rightarrow J'$		$2F_1$	$2F_2$	$2F$	$2F_1'$	$2F_2'$	$2F'$	Observed (MHz)	Calculated (MHz)	Difference (kHz)
2	3	5	6	8	7	8	10	5 856.5740	5 856.5780	−4.0
		7	6	4	9	8	6	5 856.7137	5 856.7160	−2.3
		7	6	8	9	8	10			
		5	4	4	7	6	6			
		7	8	10	9	10	12	5 856.8119	5 856.8156	−3.7
		7	8	8	9	10	10			
		7	4	4	9	6	6			
		7	10	8	9	12	10	5 856.9279	5 856.9284	−0.5
		5	8	6	7	10	8	5 857.0395	5 857.0392	0.3
		5	8	10	7	10	12			
		5	8	8	7	10	10	5 857.0665	5 857.0537	12.8
		5	2	4	7	4	6	5 857.1040	5 857.1096	−5.6
3	4	5	8	6	7	10	8	7 807.2187	7 807.2190	−0.3
		5	8	10	7	10	12			
		5	2	4	7	4	6			
		7	6	4	9	8	6	7 808.2831	7 808.2886	−5.5
		7	8	10	9	10	12			
		7	8	8	9	10	10			
		9	8	10	11	10	12	7 808.3202	7 808.3137	6.5
		9	8	8	11	10	10			
		9	6	8	11	8	10	7 808.3538	7 808.3620	−8.2
		9	6	6	11	8	8			
		9	10	12	11	12	14	7 808.3722	7 808.3717	0.5
		9	10	10	11	12	12			
		9	12	10	11	14	12	7 808.4308	7 808.4320	−1.2
		7	10	12	9	12	14	7 808.4901	7 808.4916	−1.5
4	5	7	10		9	12		9 758.9873	9 758.9855	1.8
		5	8		7	10				
6	7	11	14		13	16		13 660.7125	13 660.7133	−0.8
		9	12		11	14				

tions of this quantity from first principles are difficult, particularly in molecules with such small binding energies, and do not give a very physical picture of the origin of the results. We will follow here the more useful and conventional approach[14,18,19] of trying to understand the origin of the field gradient by using a few simple parameters characterizing the structural and electronic properties of the Kr and hydrogen halide subunits, and the structure of the van der Waals complex.

The sources of possible contributions to q may be divided into the following categories[14]: (1) valence electrons of the rare-gas atom, (2) distortion of the closed shells of the rare-gas atom by the hydrogen halide partner, and (3) charge distributions lying outside the rare-gas atom. For atoms participating in ordinary chemical bonds, for example the halogens Cl, Br, and I in ordinary molecules, contributions from electrons in the uncompleted valence shell account for most of the observed field gradients. Because this contribution is identically zero in a free rare-gas atom, we can expect it to be small in the very weakly bound van der Waals molecules, so that the ordinarily negligible effects of the second and third type can become important. Foley, Sternheimer, and Tycko have shown[10] that the field gradient at the nuclear site in a closed-shell system resulting from an external charge e at a distance R from the nucleus can be written $(2e/R^3)(1-\gamma_\infty)$,

TABLE VI. Spectroscopic constants of KrHCl.

Isotope	$\bar{B}_0 - 8D_J$ (MHz)	χ^{Cl} (MHz)	χ^{Kr} (MHz)	χ^{D} (MHz)
$^{83}KrH^{35}Cl$	1204.847 42(40)	−29.238(45)	5.200(100)	
$^{83}KrD^{35}Cl$	1188.010 53(60)	−40.824[a]	7.192(100)	0.1135[b]

[a] Fixed at average of the $^{82}KrD^{35}Cl$ and $^{84}KrD^{35}Cl$ values from Ref. 2.
[b] Fixed at the projection of the free $D^{35}Cl$ deuterium quadrupole coupling constant.

TABLE VII. Spectroscopic constants of XeHCl.

Isotope	$\bar{B}_0$ (MHz)	D_J (kHz)	χ^{Cl} (MHz)	χ^{Xe} (MHz)	χ^{D} (MHz)
^{132}XeD^{35}Cl	974.507 68(35)	3.4209(20)	−44.800(40)		0.1245[a]
^{131}XeH^{35}Cl	990.863 02(32)	3.796(20)	−34.76[b]	−4.641(50)	
^{131}XeD^{35}Cl	976.115 56(40)	3.4285(67)	−44.780(200)	−5.89(20)	0.1245[a]

[a] Fixed at the projection of the free D^{35}Cl deuterium quadrupole coupling constant.
[b] Fixed at the value for χ^{Cl} in ^{129}XeH^{35}Cl from Ref. 6.

where R must exceed the radius of the atom or ion. The proportionality factor γ_∞ is specific to each atom or ion, and results from the interaction of the electrons in the closed shells with the perturbing charge. Since this is a first-order effect, this same direct proportionality will hold for an electric field gradient arising from any system of external charges.

In view of our results for ^{83}KrH(D)F (Refs. 5 and 7) and ^{131}XeH^{35}Cl (Ref. 6), we will begin by analyzing contributions to field gradients at the rare-gas nuclear sites due to the direct and shielding enhanced field gradients arising from the first few electric multipole moments of the hydrogen halide bonding partners. The electric field gradient q_0 at a point (R, θ) along the radial direction outside a neutral cylindrically symmetric molecule is given by

$$q_0 = -6\mu\left\langle\frac{\cos\theta}{R^4}\right\rangle - 12Q\left\langle\frac{P_2(\cos\theta)}{R^5}\right\rangle - 20\Omega\left\langle\frac{P_3(\cos\theta)}{R^6}\right\rangle - 30\Phi\left\langle\frac{P_4(\cos\theta)}{R^7}\right\rangle - \cdots , \tag{5}$$

where μ, Q, Ω, and Φ are the electric dipole, quadrupole, etc., moments of the molecule. The brackets here indicate the expectation values in the vibrational ground state. All coordinates and moments are referred to the molecular center of mass. Provided that the electronic wave functions of the rare-gas atom and hydrogen halide do not overlap, the field gradient at the rare-gas nuclear site can be written

$$q = q_0(1-\gamma_\infty). \tag{6}$$

The contribution to χ is then given by

$$\chi = -\frac{eq_0Q(1-\gamma_\infty)}{h}. \tag{7}$$

The series for q_0 in Eq. (5) was calculated out to the third term for KrHCl, KrHF, and KrHCN using the values of R and θ listed for each molecule in Table IX, and the multipole moments for H^{35}Cl, HC^{14}N, and HF listed in Tables X–XII. The calculated values of $-eq_0/h$ and the measured χ^R values are listed in Table XIII. In Fig. 5 we have plotted χ^{Kr} as a function of $-eq_0/h$. We find a direct proportionality between χ^{Kr} and $-eq_0/h$, with a predicted value of χ^{Kr} of near zero in the absence of an external field gradient.

The most immediate problem with this analysis is the question of the convergence of the multipole expansion. In these molecules the center-of-mass separations across the van der Waals bonds are sufficiently large that the respective electronic wave functions barely overlap. In ^{83}KrD^{35}Cl, for example, the R_0 of 4.06 Å compares to the van der Waals radii of 2.0 Å and 1.80 Å for Kr and Cl, respectively. That part of the perturbing Hamiltonian giving rise to the effect parametrized by Eq. (6) is given by[20]

$$H_{\text{pert}} = -e\left(\frac{r}{R}\right)^2 P_2(\cos\theta_a)\left(\frac{3\mu\cos\theta_b}{R^2} + \frac{6QP_2(\cos\theta_b)}{R^3} + \frac{10\Omega P_3(\cos\theta_b)}{R^4} + \frac{15\Phi P_4(\cos\theta_b)}{R^5} + \cdots\right) \tag{8}$$

TABLE VIII. Spectroscopic constants of KrHCN.[a]

Isotope	$\bar{B}_0 - 8D_J$ (MHz)	χ^N (MHz)	χ^{Kr} (MHz)
^{83}KrHC^{14}N	1184.607 00(20)	−3.2630(60)	7.457(50)

[a] Reference 15.

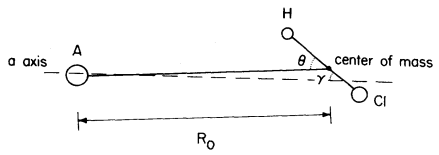

A = Kr, Xe

FIG. 3. Structural parameters for the rare-gas hydrogen chloride series of van der Waals molecules.

TABLE IX. Structural constants of KrHCl, KrHF, KrHCN, and XeHCl.

Isotope	R_0 (Å)	θ (deg.)
$^{83}KrH^{35}Cl$	4.0824	38.07
$^{83}KrD^{35}Cl$	4.0652	31.03
$^{83}KrHC^{14}N$	4.5203	27.50
$^{131}XeH^{35}Cl$	4.2456	34.76
$^{131}XeD^{35}Cl$	4.2259	28.37
$^{83}KrHF$	3.6076	39.17
$^{83}KrDF$	3.5575	31.27

for an electron in a rare-gas sheet at coordinates (r, θ_a, φ_a) (see Fig. 6) in the presence of a cylindrically symmetric charge distribution at a center-of-mass distance R, and orientation θ_b. Taking $R = 4.1$ Å, $\theta_b = 31°$, and using the multipole moments for $D^{35}Cl$, we obtain from Eq. (8), in relative importance

$$H_{\text{pert}} = 0.86 + 1.0 + 0.13 . \tag{9}$$

No experimental results are available for $\langle P_i(\cos\theta)\rangle$ for $i \geq 3$, and algebraic calculation of these terms using $\arccos(\langle\cos^2\theta\rangle)^{1/2}$ is not useful for $i \geq 4$. The behavior of these higher-order expectation values can probably be estimated using hindered-rotor wave functions for the hydrogen halide portion of the molecule. When the dominant term in the angular potential in the region being sampled by the hydrogen atom is of the form $1 - \cos\theta$, the expectation values for $P_i(\cos\theta)$ decrease monotonically to zero as i increases. For example, in $^{84}KrD^{35}Cl$, using a potential of the form 113 cm^{-1} $(1 - \cos\theta)$ with hindered rotor wave functions to describe the $D^{35}Cl$ subunit, we calculate

$$\begin{aligned} &\langle P_1(\cos\theta)\rangle = 0.85 , \\ &\langle P_2(\cos\theta)\rangle = 0.61 , \\ &\langle P_3(\cos\theta)\rangle = 0.37 , \\ &\langle P_4(\cos\theta)\rangle = 0.19 . \end{aligned} \tag{10}$$

The experimental results for the first two expectation values P_1 and P_2 are 0.88 and 0.61.[21] Algebraic expressions for P_1 through P_4 yield 0.86, 0.62, 0.29, and -0.02, respectively, for $\theta = 31.0°$. The behavior of the $\langle P_i(\cos\theta)\rangle$ values as suggested by Eq. (10), which contrasts sharply with the behavior of algebraically evaluated values of $P_i(\cos\theta), i \geq 4$, which oscillate between $+1$ and -1, is likely to make an important contribution to the very rapid convergence of the series in Eqs. (5) and (8). Using the value from (10) for $\langle P_4(\cos\theta)\rangle$ to calculate the next term of the series in Eq. (9), we obtain 0.012. Other uncertainties in applying Eq. (5) can be estimated more directly, and these are indicated as error bars in Fig. 5. Because the a inertial axis in these molecules is nearly aligned with the center-of-mass axis, errors in $\langle P_2(\cos\theta)\rangle$ will be negligible. An experimental value for $\langle P_1(\cos\theta)\rangle$ can be obtained from electric dipole measurements as[21,22]

$$\mu(\text{complex}) = \mu(\text{diatom})\langle P_1(\cos\gamma)\rangle\left(1 + \frac{2\alpha}{R_0^3}\right) , \tag{11}$$

where the hydrogen halide dipole moment is projected onto the a-axis, with a correction for the polarizability α of the rare-gas atom. Because $(\langle\cos^2\gamma\rangle)^{1/2}$ from Eq. (3) and $\langle\cos\gamma\rangle$ as obtained from Eq. (10) differ by no more than 2–3% in KrH(D)Cl,[21] and XeHCl,[23] we have chosen to cal-

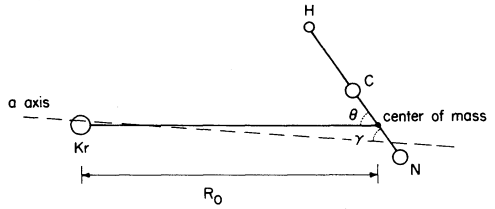

FIG. 4. Structural parameters for KrHCN. The angles θ and γ differ by 0.6°.

TABLE X. Molecular properties of $H^{35}Cl$ and $D^{35}Cl$.

	$H^{35}Cl$	$D^{35}Cl$
χ^D (MHz)[a]		0.18736
μ(D)[a]	1.1085	1.1033
Q(D Å)	3.74(12)[b]	3.74[d]
Ω(D Å^2)	2.446[c]	2.446[d]
Φ(D Å^3)	4.704[c]	4.704[d]

[a] E. W. Kaiser, J. Chem. Phys. 53, 1686 (1970).
[b] F. H. deLeeuw and A. Dymanus, J. Mol. Spectrosc. 48, 427 (1973).
[c] Reference 33.
[d] Fixed at corresponding $H^{35}Cl$ value.

TABLE XI. Molecular properties of $HC^{14}N$.

μ(D)[a]	2.9846
Q(D Å)[b]	2.42(60)
Ω(D Å^2)[c]	6.366
Φ(D Å^3)[c]	6.422

[a] A. Maki, J. Phys. Chem. Ref. Data 3, 231 (1974).
[b] Average of calculated values of 2.12 D Å, J. Tyrrell, J. Phys. Chem. 83, 2907 (1979), 2.03 D Å, Ref. 34, and an experimental value of 3.1(6) D Å measured for $HC^{15}N$ by S. L. Hartford, W. C. Allen, C. L. Norris, E. F. Pearson, and W. H. Flygare, Chem. Phys. Lett. 18, 153 (1968).
[c] Reference 34.

TABLE XII. Molecular properties of HF and DF.

	HF	DF
μ(D)[a]	1.8265	1.8188
Q(D Å)[a]	2.36(3)	2.32
Ω(D Å^2)	1.699[b]	1.699[c]
Φ(D Å^3)	1.804[b]	1.804[c]

[a] See Ref. 7.
[b] Reference 33.
[c] Values for DF assumed to be identical to those for HF.

culate $\langle\cos\theta\rangle$ algebraically from $\langle P_2(\cos\gamma)\rangle$. Except in the case of KrHCN, errors in the hydrogen halide molecular quadrupole moment contribute uncertainties in q of 1–2%. Errors arising from the neglect of terms higher than $P_3(\cos\theta)$ when calculating Eq. (5) have been estimated as

$$\frac{20\Omega\langle P_2(\cos\theta)\rangle}{R_0^6}. \tag{12}$$

With these qualifications considered we take up the physical interpretation of the curve in Fig. 5. Within the uncertainties assigned to the calculated values of $-eq_0/h$, the effect is first order, as is expected from the estimated importance of dipole polarization[6,10] and second-order quadrupole shielding effects.[10] A linear least squares fit to the data in Fig. 5 yields a slope of 21.2 ± 4 b, and a frequency axis intercept of 0.376 ± 1.6 MHz. The estimated uncertainties in the slope and intercept include the uncertainties in the values of $-eq_0/h$.

The direct proportionality observed here between q and q_0 can readily be understood qualitatively as arising from Sternheimer-type quadrupolar shielding occurring in the Kr atom. We emphasize however, that we do not know enough about the very short range parts of the Kr and hydrogen halide interaction to be able to reliably convert this constant into γ_∞ for Kr. It is well known[10] that in the idealized case of a closed-shell system perturbed by a point charge at

TABLE XIII. Summary of measured and calculated quantities related to the rare-gas coupling constants in KrHF, KrHCl, KrHCN, and XeHCl.

Isotope	χ^R (MHz)	$-eq$ (calc)/h (MHz/b)
^{83}KrH^{35}Cl	5.20(10)	0.2629(402)
^{83}KrD^{35}Cl	7.19(10)	0.3494(570)
^{83}KrHF	10.23(8)	0.4987(575)
^{83}KrDF	13.83(13)	0.6706(880)
^{83}KrHC^{14}N	7.46(5)	0.3971(1013)
^{131}XeH^{35}Cl	−4.64(5)	0.2522(388)
^{131}XeD^{35}Cl	−5.89(20)	0.3166(504)

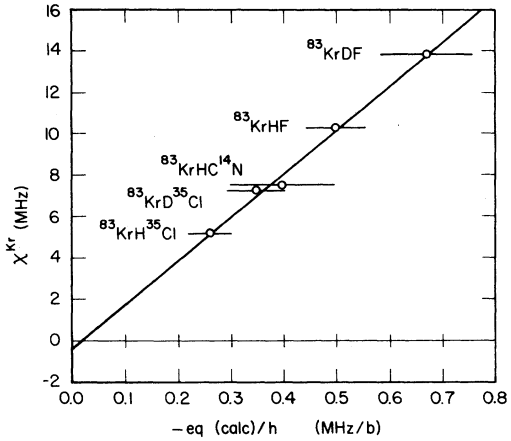

FIG. 5. Measured ^{83}Kr nuclear quadrupole coupling constant values plotted as a function of the electric field gradient at the Kr nuclear site calculated from the first few electric multipole moments of the hydrogen halide bonding partner. The slope of this line is related to the product of the quadrupole shielding of the rare-gas nucleus and the nuclear quadrupole moment, and the intercept can be related to the amount of charge transfer occurring in these systems.

distance R, the shielding parameter has a functional form $\gamma(R)$, with limiting values of $\gamma(R=0) = 0$, and $\gamma(R\to\infty)=\gamma_\infty$. For moderately heavy systems such as Cs^+, Rb^+, and Cl^-, Sternheimer *et al.* found[10] that $1-\gamma(R)$ attains approximately 70–80% of its asymptotic value of $1-\gamma_\infty$ for $R \simeq 2$ Å, with most of the contribution at $R \gtrsim 2$ Å coming from the valence p shell of the ion. Although our proportionality constant is empirically well established, it is probably related in a complicated way to the wave functions of the hydrogen halide, and to the functional form $\gamma(R)$ for the rare-gas atom.

It is still interesting to convert our slope into an effective shielding constant for Kr in the Kr-hydrogen halide systems studied here. Using Eq. (7) and the nuclear quadrupole moment of 0.27 b (Refs. 24 and 25) for the ^{83}Kr nucleus, we obtain and estimate of −77.5 ± 15 for the Kr shielding parameter, subject to the serious qualifications outlined above, and not including uncertainties

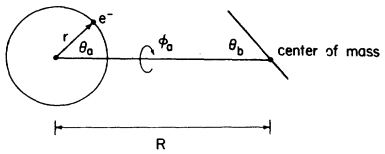

FIG. 6. Coordinate system used to parametrize the multipole expansion of the energy of an electron in a rare-gas shell at coordinate (r, θ_a, φ_a) in the field of a cylindrically symmetric system of charge at a center-of-mass distance R.

of perhaps 15% or less in the ^{83}Kr nuclear quadrupole moment measurement. Estimates of γ_∞ for Kr include a nonrelativistic variational calculation[7] including exchange effects for radial perturbations,[26] giving $\gamma_\infty = -68$, a nonrelativistic frozen-core calculation[27] giving $\gamma_\infty = -67$, estimated by those authors to be in error by perhaps 15%, not including errors arising from neglect of relativistic effects, and a calculation[28] based on relativistic Hartree-Fock-Slater electron theory, giving $\gamma_\infty = -84$. Relativistic effects have been estimated elsewhere[29] to account for approximately 7% of this last result.

The vertical axis intercept of the line in Fig. 5, (0.376 ± 1.6) MHz indicates that the combined effects of orbital overlap[30] and charge transfer from the Kr valence p orbitals is small. We may obtain an estimated upper limit to the amount of charge transferred from the Kr $4p$ orbital aligned with the molecular axis by noting that the transfer of one Kr electron out of this orbital would result in an electric field gradient at the Kr nuclear site along the a inertial axis of magnitude 750 MHz.[7] The 1.6-MHz error bound on the intercept then corresponds to a fractional electron transfer of 3×10^{-3}, or less. This result is consistent with our previous estimation[6,7] that charge transfer makes a negligible contribution to the quadrupole coupling constant in KrH(D)F.

Although the Xe data consist of only two points (see Fig. 7), they are consistent with the interpretation used for Kr. Assuming direct proportionality between χ^{Xe} and q_0 and using the ^{131}Xe nuclear quadrupole moment of -0.12 b (Refs. 31 and 32) we obtain effective quadrupole shielding constants for Xe in the ^{131}XeH^{35}Cl and ^{131}XeD^{35}Cl molecules of -152 and -154, respectively. Calculated values of γ_∞ for Xe are -138 (Ref. 6), -130 (Ref. 27), and -177 (Ref. 28), with relativistic effects accounting for about 19% of this last value.[29] That the ^{131}XeH^{35}Cl and ^{131}XeD^{35}Cl effective shielding constants agree within a few percent indicates that charge transfer has no more importance in ^{131}XeH(D)^{35}Cl than it does in the Kr systems.[6]

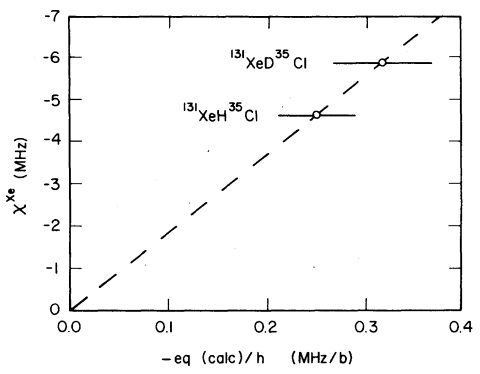

FIG. 7. Measured ^{131}Xe nuclear quadrupole coupling constant values plotted as a function of the electric field gradient at the Xe nuclear site calculated from the first few electric multipole moments of the hydrogen chloride bonding partner.

CONCLUSIONS

We have found a direct proportionality between the observed ^{83}Kr and ^{131}Xe nuclear quadrupole coupling constants in ^{83}KrH(D)^{35}Cl, ^{83}KrH(D)F, ^{83}KrHC^{14}N, and ^{131}XeH(D)^{35}Cl, and the electric field gradient at the rare-gas nuclear site along the molecular axis calculated from the electric multipole moments of the partner hydrogen halide molecule. This effect may be attributed to Sternheimer-type quadrupole shielding of the rare-gas nucleus by the electrons in the rare-gas atom. The values of the observed shielding constants are -75 for ^{83}Kr and -153 for ^{131}Xe. These constants lie within the ranges of calculated values of the Sternheimer shielding parameters γ_∞ for Kr and Xe. By using a Townes-Dailey-type argument that relates the electric field gradient at a nuclear site to the amount of "p-electron defect" in the valence shell of the atom, we find no evidence for a Lewis acid-base type transfer of electronic charge from the rare-gas atom. For ^{83}Kr the limit of uncertainty in this experiment is $\lesssim 0.003$ e. These results are consistent with our two previous analyses of the rare-gas nuclear quadrupole coupling constant in ^{131}XeH^{35}Cl (Ref. 6) and ^{83}KrH(D)F (Ref. 7).

ACKNOWLEDGMENT

The support of the National Science Foundation is gratefully acknowledged.

[1]T. J. Balle, E. J. Campbell, M. R. Keenan, and W. H. Flygare, J. Chem. Phys. 71, 2723 (1979).
[2]T. J. Balle, E. J. Campbell, M. R. Keenan, and W. H. Flygare, J. Chem. Phys. 72, 922 (1980).
[3]M. R. Keenan, E. J. Campbell, T. J. Balle, L. W. Buxton, T. K. Minton, P. D. Soper, and W. H. Flygare, J. Chem. Phys. 72, 3070 (1980).
[4]T. J. Balle and W. H. Flygare, Rev. Sci. Instrum. 52, 33 (1981).
[5]E. J. Campbell, M. R. Keenan, L. W. Buxton, T. J.

Balle, P. D. Soper, A. C. Legon, and W. H. Flygare, Chem. Phys. Lett. 70, 420 (1980).
[6]M. R. Keenan, L. W. Buxton, E. J. Campbell, T. J. Balle, and W. H. Flygare, J. Chem. Phys. 73, 3523 (1980).
[7]L. W. Buxton, E. J. Campbell, M. R. Keenan, T. J. Balle, and W. H. Flygare, Chem. Phys. 54, 173 (1981).
[8]R. M. Sternheimer, Phys. Rev. 80, 102 (1950); 84, 244 (1951); 86, 316 (1952); 95, 736 (1954).
[9]R. M. Sternheimer and H. M. Foley, Phys. Rev. 92, 1460 (1953); 102, 731 (1956).
[10]H. M. Foley, R. M. Sternheimer, and D. Tycko, Phys. Rev. 93, 734 (1954).
[11]E. J. Campbell, L. W. Buxton, T. J. Balle, and W. H. Flygare, J. Chem. Phys. 74, 813 (1981).
[12]E. J. Campbell, L. W. Buxton, T. J. Balle, M. R. Keenan, and W. H. Flygare, J. Chem. Phys. 74, 829 (1981).
[13]L. W. Buxton, E. J. Campbell, and W. H. Flygare, Chem. Phys. 56, 399 (1981).
[14]C. H. Townes and A. L. Schawlow, *Microwave Spectroscopy* (McGraw-Hill, New York, 1955).
[15]E. J. Campbell, L. W. Buxton, A. C. Legon, and W. H. Flygare (unpublished).
[16]M. R. Keenan, L. W. Buxton, E. J. Campbell, A. C. Legon, and W. H. Flygare, J. Chem. Phys. 74, 2133 (1980).
[17]M. R. Keenan, D. B. Wozniak, and W. H. Flygare, J. Chem. Phys. (in press).
[18]C. H. Townes and B. P. Dailey, J. Chem. Phys. 17, 782 (1949).
[19]E. A. C. Lucken, *Nuclear Quadrupole Coupling Constants* (Academic, New York, 1968).
[20]J. O. Hirschfelder, C. F. Curtiss, and R. B. Bird, *Molecular Theory of Gases and Liquids* (Wiley, New York, 1954).
[21]A. E. Barton, T. J. Henderson, P. R. R. Langridge-Smith, and B. J. Howard, Chem. Phys. 45, 429 (1980).
[22]S. E. Novick, P. Davies, S. J. Harris, and W. Klemperer, J. Chem. Phys. 59, 2273 (1973).
[23]K. V. Chance, K. H. Bowen, J. S. Winn, and W. Klemperer, J. Chem. Phys. 70, 5157 (1979).
[24]W. L. Faust and L. Y. Chow Chiu, Phys. Rev. 129, 1214 (1963).
[25]X. Husson, J-P. Grandin, and H. Kucal, J. Phys. B 12, 3883 (1979).
[26]P. G. Khubchandani, R. R. Sharma, and T. P. Das, Phys. Rev. 126, 594 (1962).
[27]R. P. McEachran, A. D. Stauffer, and S. Greita, J. Phys. B 12, 3119 (1979).
[28]F. D. Feiock and W. R. Johnson, Phys. Rev. 187, 39 (1969).
[29]K. D. Sen and P. T. Narasimham, Phys. Rev. B 15, 95 (1977).
[30]T. P. Das and M. Karplus, J. Chem. Phys. 42, 2885 (1965).
[31]A. Bohr, J. Koch, and E. Rasmussen, Ark. Fys. 4, 455 (1952).
[32]W. L. Faust and M. N. McDermott, Phys. Rev. 123, 198 (1961).
[33]D. Maillard and B. Silvi, Mol. Phys. 40, 933 (1980).
[34]J. E. Gready, G. B. Bacskay, and N. S. Hush, Chem. Phys. 31, 467 (1968).